Subjective value, not a grid-like code, describes neural activity in ventromedial prefrontal cortex during value-based decision-making

Sangil Lee[1†*], Linda Q. Yu[12†], Caryn Lerman[3], and Joseph W. Kable[1]

[1]Department of Psychology, University of Pennsylvania, Philadelphia, PA, 19104 USA

[2]Carney Institute for Brain Science, Brown University, Providence, RI, 02912 USA

[3]Norris Comprehensive Cancer Center, University of Southern California, Los Angeles, CA, 90033, USA

† These two are co-first authors and are listed in alphabetical order

* Correspondence: sangillee3rd@gmail.com

Abstract

Across numerous studies, ventromedial prefrontal cortex (vmPFC) activity has been found to correlate with subjective value during value-based decision-making. Recently, however, vmPFC has also been shown to reflect a grid-like code used for navigation through physical and conceptual space. This raises the possibility that such a grid-like code could broadly underlie vmPFC's role in complex cognition and, specifically, may be used for comparing options in decision-making. Here, we first show that, in theory, a grid-like code could account for vmPFC activity previously attributed to subjective value. We then test for grid-like modulation in a large fMRI dataset of intertemporal choice. Here, however, we find that the grid-like model fails confirmatory tests and that instead subjective value provides the better description for vmPFC responses. Our results constrain the tasks for which grid-like modulation is observed in vmPFC and suggest that vmPFC might implement the most useful code for the current task.

Keywords: vmPFC, valuation, grid cell, hexagonal modulation

Many studies in decision neuroscience have identified a critical role for the ventromedial prefrontal cortex (vmPFC) in decision-making. Specifically, neural activity in the vmPFC correlates with the subjective value of expected or experienced outcomes across a wide variety of different decision-making tasks and different categories of outcomes[1–3]. Neural correlates of subjective value have been found in vmPFC using both fMRI in humans as well as single cell recording in non-human animals[4–8]. One interpretation of these results is that vmPFC encodes the subjective value of potential outcomes, which is then used to make choices between outcomes[9,10].

However, recent human neuroimaging studies have suggested that a similar area of vmPFC serves a different function, encoding representations that enable navigation through real and conceptual spaces[11–13]. Both intracortical recordings and fMRI studies of humans navigating virtual arenas have shown that activity in medial prefrontal cortex responds to different spatial locations in a hexagonally symmetric pattern characteristic of grid cells[12–15]. Grid cells were first discovered in entorhinal cortex (ERC) during spatial navigation and provide an efficient representation of two-dimensional space[12,16,17]. More recently, fMRI signatures of a grid-like code have been observed in vmPFC during navigation in a purely conceptual space[11]. Specifically, stimuli in that study were defined along two dimensions, and when subjects imagined a stimulus transforming through the conceptual space defined by those two dimensions, activity in vmPFC showed a similar response pattern as that observed during two-dimensional spatial navigation.

These recent results have led some to speculate that grid-like codes might account for the role of vmPFC in complex cognition generally, as the basic underpinnings of cognitive maps, including during decision-making[18]. For example, during decision making, many choices are

between two options that differ along two dimensions – for example, gambles that differ in risk and payoff, foods that differ in health and taste, or goods that differ in quality and price. Might vmPFC activity during decision-making reflect navigation through a conceptual space defined by these attribute dimensions? If true, grid-like codes could provide a general account of vmPFC function across multiple domains.

Here we test whether grid-like responses reflecting conceptual navigation through attribute space can account for the activity observed in vmPFC during decision making. We first show theoretically that a grid-like code could in principle explain activity correlated with subjective value, as a plausible construction of grid-like responses for a two-attribute choice task is highly correlated with subjective value. We then empirically test which of these two models better explains BOLD activity in vmPFC, concentrating on out-of-sample predictions, using a large existing dataset of subjects performing a standard intertemporal choice task[19]. Our results unambiguously show that vmPFC activity in this task is correlated with subjective value and cannot be explained by grid-like modulation. This finding has important implications for attempts to build a general theory of vmPFC function.

Results

Here we compare two potential coding schemes for vmPFC during decision-making, subjective value and grid-like modulation, both of which are functions of the two attribute dimensions of the choice options. In the intertemporal choice task we study, participants choose on every trial between an immediate option, which is fixed at $20 on every trial, and a delayed option, which varies from trial to trial in monetary amount and length of delay (**Fig. 1a**). This design simplifies the identification of neural correlates of subjective value, as only the subjective value of the delayed option needs to be considered; since the immediate option is fixed, the sum,

difference or ratio of the subjective values of the two options are all linearly related to the subjective value of the delayed option. Subjective values are idiosyncratic, as they depend on how individual subjects weight the two attribute dimensions (i.e., their discount rate for delayed rewards), but all subjects prefer larger magnitudes and smaller delays, leading to the highest response in one corner of the two-dimensional attribute space. For grid-like modulation, we assume that the relevant conceptual navigation in this task involves "traversing" between the two options being considered (**Fig. 1b**). Since the immediate option is fixed and the delayed option is always larger in amount and longer in delay, this restricts the possible angles of "travel" to ninety degrees. A grid-like code would lead to peaks in activity when navigating along hexagonally symmetric directions spaced sixty degrees apart, with the angle of these peak directions (the grid angle) being the one free parameter. For example, a person with a grid-angle at 0 degrees would have activity peaks at 0 and 60 degrees of traversing and troughs at 30 and 90 degrees.

We first show via simulation that grid-like modulation over decision attribute space could in theory account for previously observed neural correlates of subjective value in this task[4,19–21]. Starting from the assumptions above, we calculated the best-fitting grid angle for different subjective value landscapes generated assuming different intertemporal preferences (i.e., different discount rates for delayed rewards). **Fig. 2** shows subjective value signals and their best-fitting grid-like signals at various discount rates. The maximum correlation between the two signals ranges between $r = 0.5$ and $r = 0.7$ depending on the discount rate. These high correlations suggest that it is possible for grid-like modulation and subjective value to be confused with each other, and therefore grid-like modulation could in theory be a possible alternative account of previously reported activity correlated with subjective value.

To determine which of these alternatives best accounts for vmPFC activity during decision-making, we turned to a large existing fMRI dataset of participants making intertemporal choices. Critically, participants in this study completed intertemporal choices in two sessions on separate days, permitting us to perform the same exact test for a grid-like code as that performed in Constantinescu et al. (2016): consistency of grid angle across sessions.

First, using the first session's data, we confirmed that vmPFC activity was correlated with both subjective value and grid-like modulation signals, as expected given our simulation results above. **Fig. 3** shows significant effects across the whole brain for both subjective value and grid-like modulation regressors in session 1 data. Perhaps given the statistical power in our dataset (n = 107), we observed significant effects in widespread brain regions for both analyses. In fact, we found that almost the entire brain reaches statistical significance for the grid-like modulation signal (*i.e.*, the *F*-test of the two grid angle regressors). This includes peaks in the vmPFC and entorhinal cortex (ERC) as observed previously during conceptual navigation by Constantinescu et al. (2016). The subjective value effects, which we have reported previously for this dataset[19], are somewhat more circumscribed, and include peaks in the vmPFC and ventral striatum (VS) that overlap with previous meta-analyses of subjective value correlates during decision-making[1].

The widespread effects observed in the first session for the grid-like modulation analysis emphasize an important point: given that the angle of grid modulation is a free parameter, this analysis provides a good degree of flexibility to fit a diversity of response patterns. Recognizing this, Constantinescu et al. (2016) argue that the critical test for grid-like responses fixes this angle for the second session based on the first session's data, and then shows that 6-fold modulation around this angle, as predicted by a grid-like pattern, is stronger than modulations at

other folds. Thus, we next turned to an analysis of grid angle consistency in our second session's data. For this analysis, we defined two grid cell regions-of-interest (ROIs) based on the peaks in vmPFC and ERC in Constantinescu et al. (2016) and two subjective value ROIs in vmPFC and VS based on the meta-analysis in Bartra et al. (2013).

Our grid angle consistency analysis unambiguously showed that vmPFC activity is consistent with subjective value, and does not exhibit consistent grid-like modulation, regardless of how the vmPFC ROI is defined (**Fig. 4**). We simulated the results of the grid angle consistency analysis assuming the underlying signal is subjective value and assuming the underlying signal is grid-like modulation. If the underlying signal is subjective value, the angle consistency analysis should show decreasing effects from 4 to 8 fold. In contrast, if the underlying signal is grid-like modulation, then the largest effect should be for the 6-fold regressor. None of the ROIs show the predicted pattern for a grid-like code. Both vmPFC ROIs and the VS ROI show the pattern expected for a subjective value signal.

Discussion

Here we tested whether vmPFC activity during decision-making, which has previously been shown to correlate with subjective value, could instead be better explained by grid cell-like activity reflecting conceptual navigation through the space defined by the attributes of the choice options. This idea is theoretically plausible, as there can be a high correlation between subjective value and grid-like modulation signals. Using the methods from Constantinescu et al. (2016), we tested for grid-like responses in vmPFC in a large fMRI dataset of a standard two-attribute decision task (ITC) involving two sessions. The critical test for a grid-like code involves fixing the subject-specific grid angle for a given region based on the first session's data and testing in the second session for significant 6-fold modulation at that grid angle, which is also larger than

modulation at that grid angle for all other number of folds. Activity in vmPFC during decision making unambiguously failed this critical test. Rather, the pattern that was observed in this analysis of grid angle consistency was exactly what one would expect if the true underlying signal was subjective value. Thus, we found no evidence for a grid-like code in vmPFC during decision-making, and subjective value remains the best description of decision-related activity in vmPFC.

Our results constrain the implications of Constantinescu et al. (2016) by limiting the conditions under which a grid-like code is observed in the vmPFC. Our intertemporal choice task is obviously very different from the sort of mental navigation demanded in Constantinescu et al. (2016). Their study involved extensive learning of a novel conceptual space by the participants prior to the navigational task; ours takes advantage of a spontaneous conceptual space created by the option attributes as they are presented in a choice task. Their navigational task involved a period of mental simulation where the participants are asked to imagine the progress of the stimulus, akin to virtual navigation, whereas we simply ask participants to make a choice. Nevertheless, the two tasks share important similarities in that both operate within a two-dimensional space where grid-like representations of the task structure might be expected and indeed have been proposed[18]. Our findings suggest that the two-dimensional space defined by the option attributes that is available during decision-making does *not* provoke grid-like representations, and thus a grid-like code cannot explain neural activity in the vmPFC during decision-making tasks.

The vmPFC is important for a wide variety of functions, from learning and decision-making to schematic memory and social cognition[22–28]. A possible explanation for this diversity is that different subregions of the vmPFC serve different functions. Though we used the same

ROI as in Constantinescu et al. (2016) for our analysis, fMRI does not allow for the resolution necessary to differentiate between populations of neurons that may have different functions. Therefore, one possibility is that different neuronal populations in the vmPFC underlie grid-like and subjective value responses in different environments. However, another possibility is that the vmPFC represents the *relevant* cognitive map for the current task[29–31], and therefore the nature of the coding scheme in vmPFC may depend on the demands of the task at hand. A decision-maker does not necessarily need to know the spatial relationships between different choice options in attribute space. In contrast, subjective value is a representation that has long been known to afford useful features for decision-making; for example, using such a representation of multi-attribute options and choosing the maximal valued option is guaranteed to result in transitive, non-cyclical choices[32]. Subjective value may therefore be the most efficient representation of the option space for the kind of decision tasks we studied here.

Methods

Dataset

We used an fMRI dataset from Kable et al. (2017). The dataset can be obtained by contacting the corresponding author of the paper. Participants completed two sessions in which they performed an intertemporal choice task in the scanner 10 weeks apart. In each scan session, participant made 120 binary choices between a smaller immediate reward and a larger later reward. The smaller immediate reward was held constant at $20 today while the larger later reward varied in amount (A: $21 ~ $85) and delay ($D$: 20 days ~ 180 days) from trial to trial. Each trial displayed the amount and delay of the larger later option on the screen; the constant immediate option was not displayed. Participants used a button pad to indicate whether they would like to accept the larger delayed option shown on the screen or to reject it in favor of the

smaller immediate option. Of the 160 non-pilot participants that completed session 1, we excluded participants with any missing runs (n = 6), too much head movement (any run out of 4 runs with >5% of mean image displacements greater than 0.5mm; n = 3), more than 3 missing trials per run for two or more runs (n = 2), and one participant who expressed knowledge of his experimental condition. From the remaining 148, only 114 also completed session 2, from which we also excluded those with missing runs (n = 3), head movement (n = 2), or too many missing trials (n = 2). Finally, we also removed 5 participants from further analyses as their choices were entirely one-sided (i.e., always chose the delayed option or always chose the immediate option in either session). This gave us a total of 102 participants, each with 2 sessions of data.

Participants were scanned with a Siemens 3T Trio scanner with a 32-channel head coil. T1-weighted anatomical images were acquired using an MPRAGE sequence (T1 = 1100ms; 160 axial slices, 0.9375 x 0.9375 x 1.000 mm; 192 x 256 matrix). T2*-weighted functional images were acquired using an EPI sequence with 3mm isotropic voxels, (64 x 64 matrix, TR = 3,000ms, TE = 25ms; tilt angle = 30°) involving 53 axial slices with 104 volumes. B0 fieldmap images were also collected for distortion correction (TR = 1270ms, TE = 5 and 7.46ms). The datasets were preprocessed via FSL FEAT (FMRIB fMRI Expert Analysis Tool). Functional images were skull stripped with BET (FMRIB Brain Extraction Tool), motion corrected and aligned with MCFLIRT (FMRIB Linear Image Restoration Tool with Motion Correction), spatially smoothed with a FWHM 9mm Gaussian Kernel, and high pass filtered (104sec cutoff). Registration was performed with FNIRT with warp resolution of 20mm (FMRIB's Non-linear Image Registration Tool) to a 2mm MNI standard brain template.

Correlation between subjective value and grid regressors

First, we sought to show that, in theory, hexagonally-symmetric grid-like modulation could mimic or account for activity correlated with subjective value during decision making. To do this, we simulated a subjective value signal at a given discount rate for a range of amounts and delays, and then estimated the best-fitting grid-like modulation for this signal. For a given discount rate, the subjective values of delayed monetary outcomes were calculated using the hyperbolic model:

$$SV\ of\ \$A\ in\ D\ days\ = \frac{A}{1+kD} \quad (1)$$

where k is the discount rate. The amount A varied from 20 to 80 in increments of 2 (31 levels) and the delay D varied from 20 to 180 in increments of 5 (33 levels) resulting in a total of 1023 subjective values for a given k. This 1023-element vector (SV) was then regressed against two grid-like modulation regressors in order to estimate the best-fitting grid-like modulation signal:

$$SV_t = \beta_0 + \beta_1 \cos(6\theta_t) + \beta_2 \sin(6\theta_t) + \epsilon_t, \qquad \theta_t = \text{atan}\left(\frac{A_t - 20}{D_t}\right) \quad (2)$$

The model contains a linear combination of the sine and cosine of the trajectory angle θ with 60° periodicity. The trajectory angle θ is taken as the angle between the abscissa and the line between the immediate option ($20 now) and the delayed option ($$A$ in D days) in the two-dimensional space defined by the amount and delay attributes, for each trial t. We calculated the Pearson correlation between SV and the fitted signal to assess the similarity between the two. This procedure was repeated for 51 levels of k whose base-10 log ranged from -5 (i.e., k = 0.00001) to 0 (i.e., k = 1) in 0.1 increments.

fMRI analysis

We first performed two GLMs on session 1 data to show that vmPFC activity was correlated with both subjective value and grid-like modulation signals. For the subjective value

GLM, we used two regressors of interest: an event regressor that modeled average activity of all trials, and second regressor that modeled activity correlated with the subjective value of the variable delayed reward across trials. The subjective value of the delayed reward was estimated by fitting a hyperbolic discounting model to choice data (each session separately) using logistic regression (eq. 3; A is the delayed amount, D is the delay, k is the discount rate, and β is the scaling factor).

$$logit\big(P(choice = delayed)\big) = \beta\left(\frac{A}{1 + kD} - 20\right) \quad (3)$$

The between-session correlation of *logk* was 0.74, suggesting that the discount rates were very stable across the 10-week period. For the grid-like modulation GLM, we used three regressors: an event regressor and two hexagonal grid angle regressors ($\cos(6\theta_t)$, $\sin(6\theta_t)$, where $\theta_t = \text{atan}\big((A_t - 20)/D_t\big)$). The F-statistic of the two hexagonal grid regressors was converted to z-statistic for significance testing. Each participant's z-converted F-statistics were used to perform permutation testing against the null (by sign-flipping) with threshold-free cluster enhancement at the group-level. We also defined spherical ROIs from peak GLM coordinates in these two analyses closest to the vmPFC and ERC peaks in Constantinescu et al. (2016) and to the vmPFC and VS peaks in Bartra et al. (2013). Results in these ROIs were the same as for the ROIs reported above and are presented in the supplemental materials.

The key feature that identifies a grid-like code in fMRI is grid angle consistency. This means that the hexagonal grid for a given region in a given person has its unique orientation angle that stays constant across time. For example, when people are navigating through a two dimensional space, one person's may have 6-fold modulating activity that peaks when the person traverses through space at 20 + 60x (x = 0 … 5) degree angles while another person's activity may peak at 40 + 60x (x = 0 … 5) degree angles. Hence demonstrating the consistency of this

unique grid angle across different scan sessions is the key test of a grid-like code. We tested grid angle consistency in regions of interest defined based on a previous reports of a grid-like code during conceptual navigation, as well as in regions of interest defined based on meta-analysis of subjective value correlates during decision making. For the former, we created two spherical ROIs (radius = 2 voxels) from the peak activation coordinates reported by Constantinescu et al. (2016) in vmPFC and ERC. For the latter, we adopted the vmPFC and VS ROIs from the Bartra et al. (2013) meta-analysis.

The *n*-fold grid-angle for the consistency analysis was first calculated from a GLM on the first session's data that included $\cos(n\theta)$ and $\sin(n\theta)$ as regressors. The average coefficients in each the ROI ($\bar{\beta}_{cos}, \bar{\beta}_{sin}$) were used to calculate that individual's *n*-fold grid angle ($\phi_n = \text{atan}\left(\bar{\beta}_{sin}/\bar{\beta}_{cos}\right)/n$) for that ROI. Then, for the GLM on the second session's data, we used the following consistency regressor:

$$\cos\left(n\left(\theta_t - \phi_n\right)\right), \theta_t = \text{atan}\left(\frac{A_t - 20}{D_t}\right) \quad (4)$$

The average *z*-statistic of this consistency regressor within the pre-defined ROIs was used to measure the consistency effect across sessions. The key test was whether the consistency effect was significant and greatest at 6-fold.

We simulated the results of this grid angle consistency analysis under two conditions: when the underlying signal is subjective value, and when the underlying signal is 6-fold grid-like modulation. For subjective value, we calculated the 102 subjects' subjective values in both session 1 and session 2 via eq. 3 and performed the angle consistency analysis outlined above. For 6-fold modulation, we picked a random angle between 0 and 60 degrees for each subject, simulated a 6-fold modulation signal according to eq. 4 (with $n = 6$), and then performed the angle consistency analysis.

Acknowledgements: This study was funded by grants from the National Cancer Institute R01 CA170297 (JK, CL) and R35 CA197461 (CL)

Author Contributions: Conceptualization, L.Q.Y; Methodology and Formal Analysis, S.L; Investigation, all authors; Writing - Original Draft, S.L. and L.Q.Y.; Writing Review & Editing, all authors; Supervision J.W.K.; Funding Acquisition C.L., and J.W.K.

Declaration of Interests: The authors declare no competing interests.

References

1. Bartra, O., McGuire, J. T. & Kable, J. W. The valuation system: A coordinate-based meta-analysis of BOLD fMRI experiments examining neural correlates of subjective value. *Neuroimage* **76**, 412–427 (2013).

2. Clithero, J. A. & Rangel, A. Informatic parcellation of the network involved in the computation of subjective value. *Soc. Cogn. Affect. Neurosci.* (2013). doi:10.1093/scan/nst106

3. Levy, D. J. & Glimcher, P. W. The root of all value: A neural common currency for choice. *Curr. Opin. Neurobiol.* **22**, 1027–1038 (2012).

4. Kable, J. W. & Glimcher, P. W. The neural correlates of subjective value druing intertemporal choice. *Nat. Neurosci.* **10**, 1625–1633 (2007).

5. Strait, C. E., Blanchard, T. C. & Hayden, B. Y. Reward value comparison via mutual inhibition in ventromedial prefrontal cortex. *Neuron* (2014). doi:10.1016/j.neuron.2014.04.032

6. Yamada, H., Louie, K., Tymula, A. & Glimcher, P. W. Free choice shapes normalized value signals in medial orbitofrontal cortex. *Nat. Commun.* (2018). doi:10.1038/s41467-017-02614-w

7. McNamee, D., Rangel, A. & O'Doherty, J. P. Category-dependent and category-independent goal- value codes in human ventromedial prefrontal cortex. *Nat. Neurosci.* **16**, 479–485 (2013).

8. Howard, J. D., Gottfried, J. A., Tobler, P. N. & Kahnt, T. Identity-specific coding of future rewards in the human orbitofrontal cortex. *Proc. Natl. Acad. Sci. U. S. A.* (2015). doi:10.1073/pnas.1503550112

9. Kable, J. W. & Glimcher, P. W. The Neurobiology of Decision: Consensus and Controversy. *Neuron* (2009). doi:10.1016/j.neuron.2009.09.003

10. Rich, E. L. & Wallis, J. D. Decoding subjective decisions from orbitofrontal cortex. *Nat. Neurosci.* (2016). doi:10.1038/nn.4320

11. Constantinescu, A. O., O'Reilly, J. X. & Behrens, T. E. J. Organizing conceptual knowledge in humans with a gridlike code. *Science (80-.).* (2016). doi:10.1126/science.aaf0941

12. Doeller, C. F., Barry, C. & Burgess, N. Evidence for grid cells in a human memory network. *Nature* (2010). doi:10.1038/nature08704

13. Jacobs, J. *et al.* Direct recordings of grid-like neuronal activity in human spatial navigation. *Nat. Neurosci.* (2013). doi:10.1038/nn.3466

14. Bao, X. *et al.* Grid-like Neural Representations Support Olfactory Navigation of a Two-Dimensional Odor Space. *Neuron* (2019). doi:10.1016/j.neuron.2019.03.034

15. Nau, M., Navarro Schröder, T., Bellmund, J. L. S. & Doeller, C. F. Hexadirectional coding of visual space in human entorhinal cortex. *Nat. Neurosci.* (2018). doi:10.1038/s41593-017-0050-8

16. Hafting, T., Fyhn, M., Molden, S., Moser, M.-B. & Moser, E. I. Microstructure of a spatial map in the entorhinal cortex. *Nature* (2005). doi:10.1038/nature03721

17. Behrens, T. E. J. *et al.* What Is a Cognitive Map? Organizing Knowledge for Flexible Behavior. *Neuron* (2018). doi:10.1016/j.neuron.2018.10.002

18. Bellmund, J. L. S., Gärdenfors, P., Moser, E. I. & Doeller, C. F. Navigating cognition: Spatial codes for human thinking. *Science (New York, N.Y.)* (2018). doi:10.1126/science.aat6766

19. Kable, J. W. *et al.* No Effect of Commercial Cognitive Training on Brain Activity, Choice Behavior, or Cognitive Performance. *J. Neurosci.* **37**, 7390–7402 (2017).

20. Kable, J. W. & Glimcher, P. W. An 'as soon as possible' effect in human intertemporal decision making: Behavioral evidence and neural mechanisms. *J. Neurophysiol.* (2010). doi:10.1152/jn.00177.2009

21. Cox, K. M. & Kable, J. W. BOLD Subjective Value Signals Exhibit Robust Range Adaptation. *J. Neurosci.* **34**, 16533–16543 (2014).

22. Lieberman, M. D., Straccia, M. A., Meyer, M. L., Du, M. & Tan, K. M. Social, self,(situational), and affective processes in medial prefrontal cortex (MPFC): causal, multivariate, and reverse inference evidence. *Neurosci. Biobehav. Rev.* (2019).

23. Roy, M., Shohamy, D. & Wager, T. D. Ventromedial prefrontal-subcortical systems and the generation of affective meaning. *Trends in Cognitive Sciences* (2012). doi:10.1016/j.tics.2012.01.005

24. Gilboa, A. & Marlatte, H. Neurobiology of Schemas and Schema-Mediated Memory. *Trends in Cognitive Sciences* (2017). doi:10.1016/j.tics.2017.04.013

25. Janowski, V., Camerer, C. & Rangel, A. Empathic choice involves vmPFC value signals that are modulated by social processing implemented in IPL. *Soc. Cogn. Affect. Neurosci.* (2013). doi:10.1093/scan/nsr086

26. Powell, N. J. & Redish, A. D. Representational changes of latent strategies in rat medial prefrontal cortex precede changes in behaviour. *Nat. Commun.* (2016). doi:10.1038/ncomms12830

27. Grabenhorst, F. & Rolls, E. T. Value, pleasure and choice in the ventral prefrontal cortex. *Trends in Cognitive Sciences* (2011). doi:10.1016/j.tics.2010.12.004

28. Fehr, E. & Camerer, C. F. Social neuroeconomics: the neural circuitry of social preferences. *Trends in Cognitive Sciences* (2007). doi:10.1016/j.tics.2007.09.002

29. Wilson, R. C., Takahashi, Y. K., Schoenbaum, G. & Niv, Y. Orbitofrontal cortex as a cognitive map of task space. *Neuron* (2014). doi:10.1016/j.neuron.2013.11.005

30. Schuck, N. W., Cai, M. B., Wilson, R. C. & Niv, Y. Human Orbitofrontal Cortex Represents a Cognitive Map of State Space. *Neuron* **91**, 1402–1412 (2016).

31. Bernardi, S. *et al.* The geometry of abstraction in hippocampus and prefrontal cortex. *bioRxiv* (2018). doi:10.1101/408633

32. Samuelson, P. a. Note on Measurement of Utility. *Rev. Econ. Stud.* **4**, 155–161 (1937).

Figures

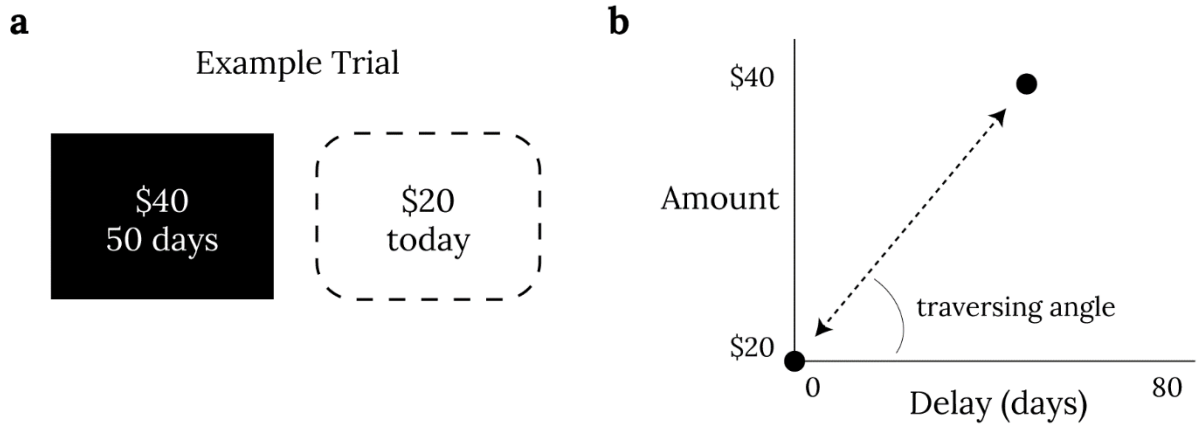

Figure 1. Example intertemporal choice trial (a) and corresponding grid model (b). Panel **a** shows an example trial of the intertemporal choice task. Participants could either choose the larger, delayed monetary reward shown on screen, or opt for the smaller immediate reward not shown on the screen (always $20). Panel **b** shows how a choice between the two options in panel **a** could be construed in terms of conceptual navigation. The two dots represent the two choice options of $20 today and $40 in 50 days. The angle of the line that connects these two options in conceptual space could be thought of as the traversing angle.

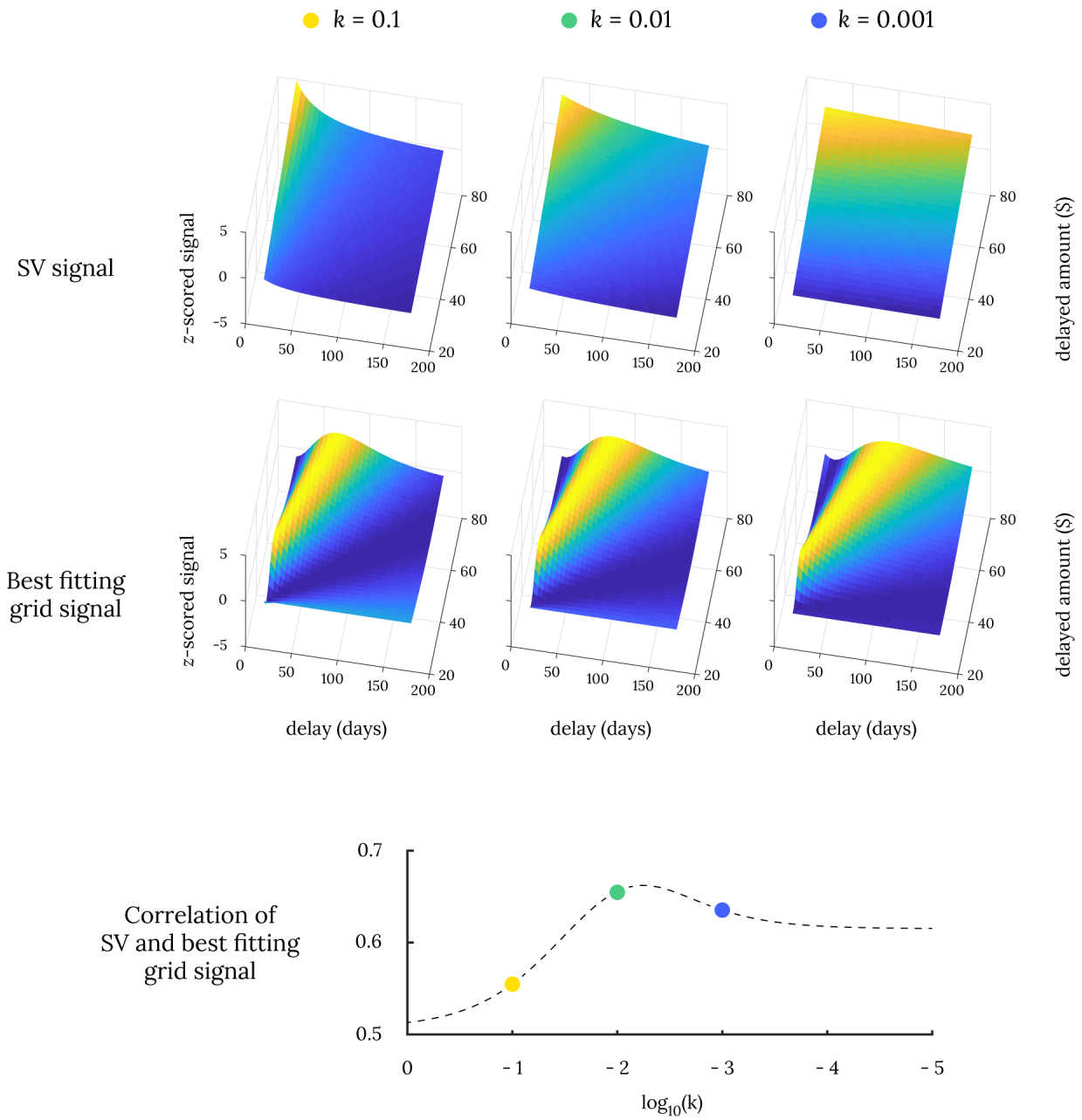

Figure 2. Correlation between SV signal and its most similar hexagonal modulation signal. The top three panels show simulated SV signal for various delayed amounts at various discount rates and the next three panels below show their respective best fitting hexagonal grid modulations. The correlation between the two signals are provided below across various discount rates.

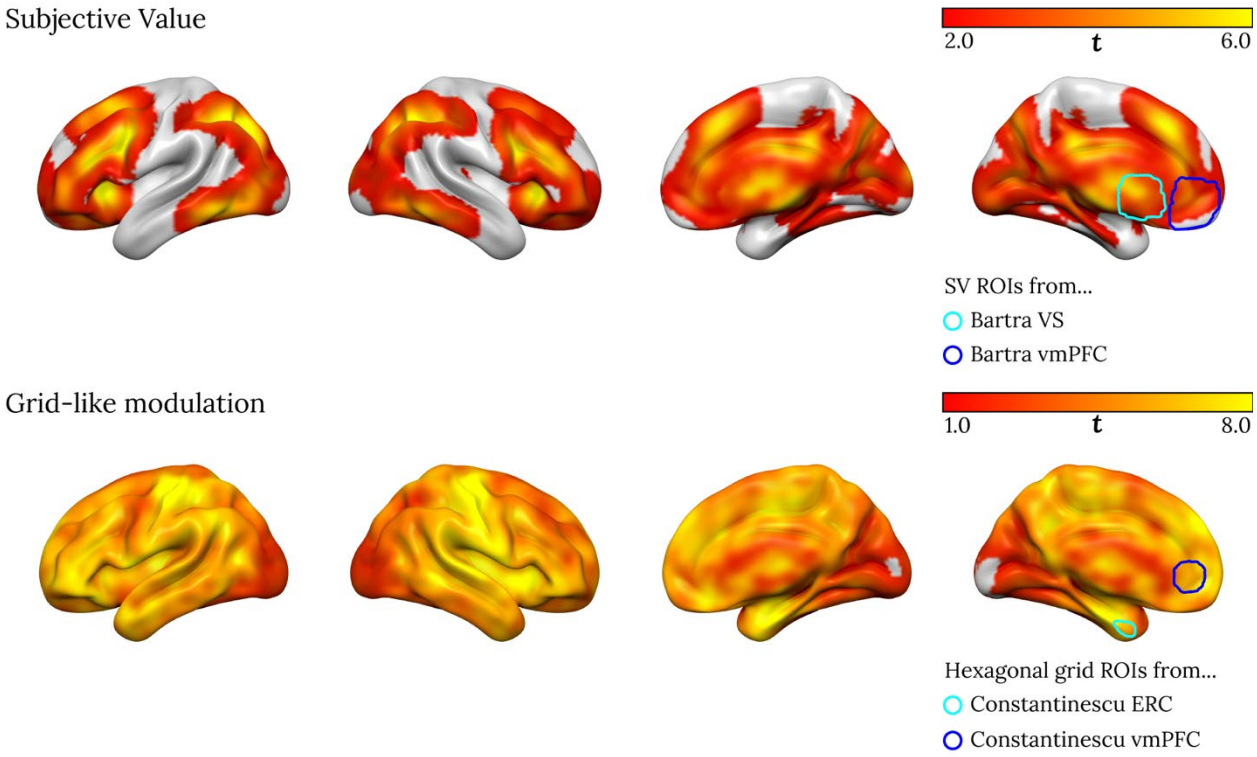

Figure 3. Regions with significant SV correlation (top) and significant grid-like modulation (bottom) in session 1. ($p < 0.05$ with permutation testing with threshold free cluster enhancement).The rightmost brain show overlays of the two ROIs from Bartra et al. (2013) on top and the two ROIs from Constantinescu et al. (2016) on bottom.

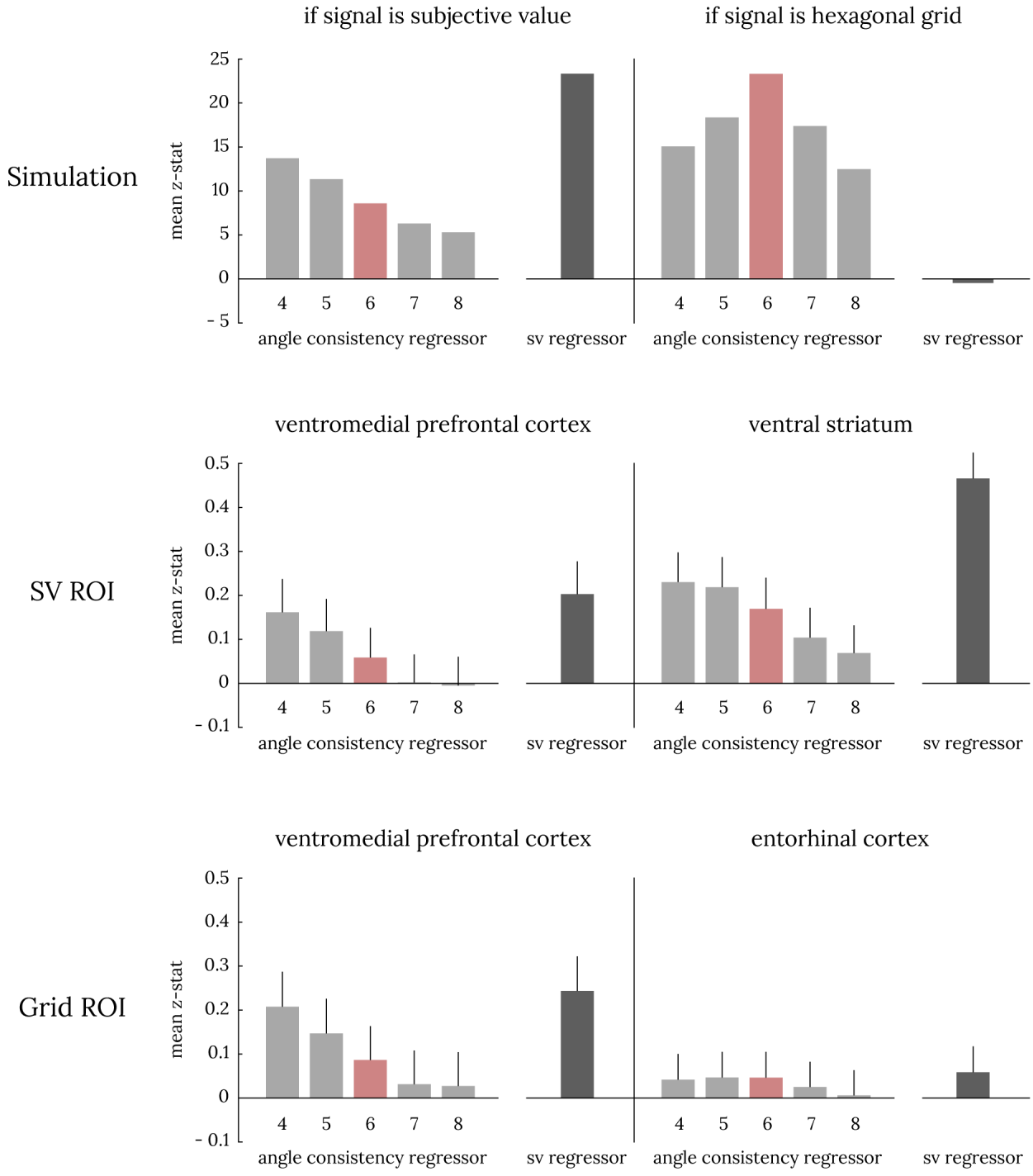

Figure 4. Grid-angle consistency effects and SV effects in session 2 data. The top two panels show simulated results of grid-angle consistency analysis when the true signal is SV (left) or a grid-like code (right). The middle two panels show the grid-angle consistency analysis and SV effects in SV ROIs from Bartra et al. (2013); the bottom two panels show them for hexagonal grid ROIs from Constantinescu et al. (2016).

Supplemental Materials

Angle consistency analysis for ROIs generated from our dataset

To address the concern that ROIs from previous studies (i.e., Bartra et al. (2013) ROIs for SV and Constantinescu et al. (2016) ROIs for hexagonal grid) may not exactly match the loci of activation in our data, we defined additional ROIs based on session 1 GLM peak statistics for SV and grid angle regressors. For the SV GLM, we created a spherical ROI around the peak for the permutation *t*-score for the SV regressor that was closest to the center of the Bartra et al. (2013) ROIs. For the grid angle GLM, we created a spherical ROI around the peak *z*-transformed *F*-statistic for the grid angle regressors that was closest to the center of the Constantinescu et al. (2016) ROIs (top panels of **Fig S.1**). We found that the SV ROIs based on *t*-statistics were entirely encapsulated by the ROIs from Bartra et al. (2013), while the hexagonal grid ROIs based on *F*-statistics were shifted slightly from the ROIs from Constantinescu et al. (2016).

Grid angle consistency analysis from these ROIs show the same pattern that we observed with Bartra et al. (2013) and Constantinescu et al. (2016) ROIs (bottom panels of **Fig S.2**). We see that the two vmPFC ROIs and the ventral striatum ROI show the pattern that is expected from an SV signal. We also see that the ERC ROI does not exhibit a pattern consistent with either SV or a grid-like code.

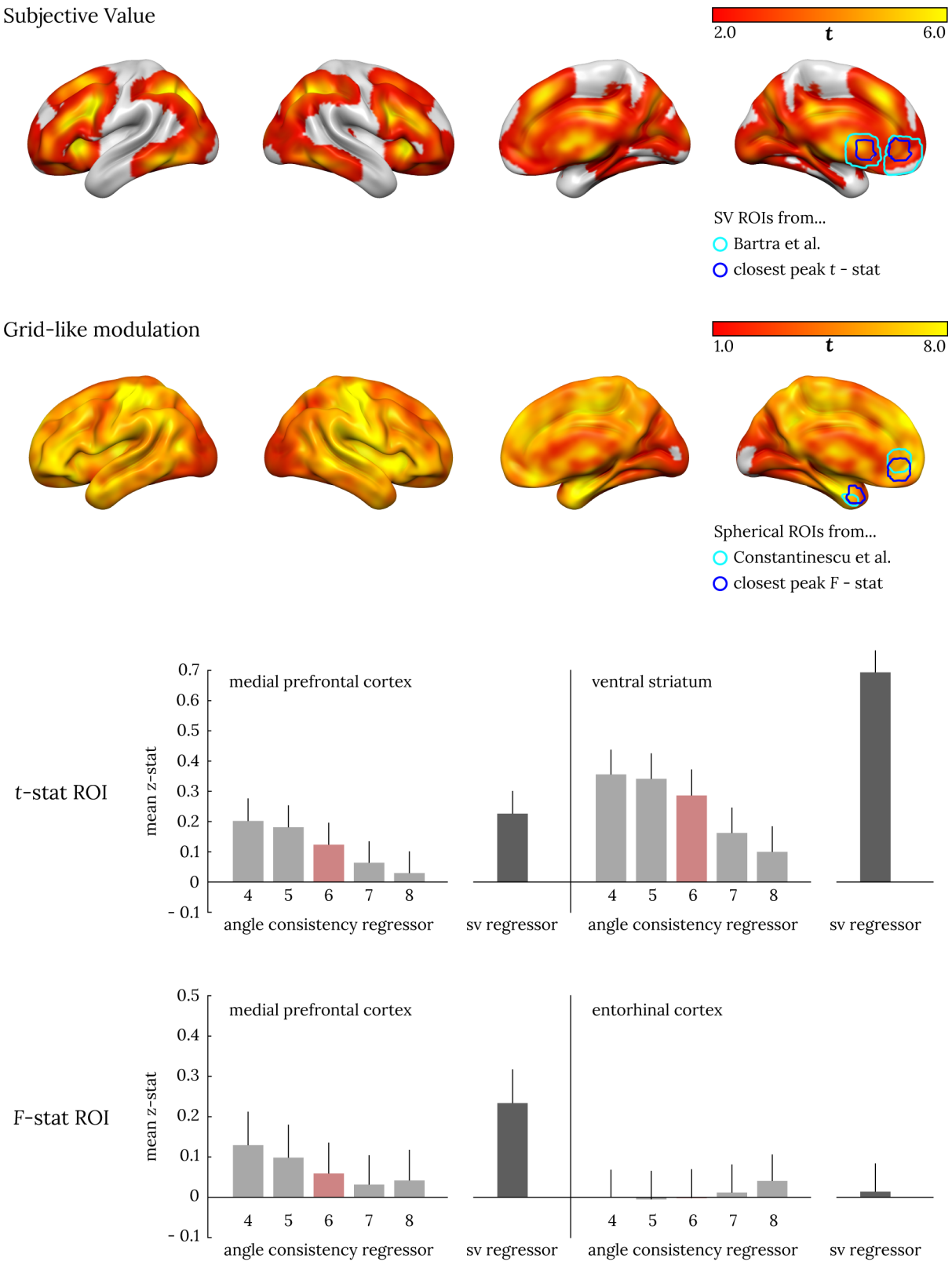

Fig. S.1. GLM-based ROIs (above) and their angle consistency analysis (below).